The corresponding author is Ann Rowan (ann.rowan@uib.no)

Increasing precipitation will partially offset the impact of warming air temperatures on glacier loss in the monsoon-influenced Himalaya until 2100 CE

Anya M. Schlich-Davies[1], Ann V. Rowan[2], Andrew N. Ross[1], Duncan J. Quincey[3], Vivi K. Pedersen[4]

[1]Priestley International Centre for Climate, School of Earth and Environment, University of Leeds, UK
[2]Department of Earth Science, University of Bergen and Bjerknes Centre for Climate Research, Bergen, Norway
[3]School of Geography, University of Leeds, UK
[4]Department of Geoscience, Aarhus University, Aarhus C, Denmark

Himalayan glaciers are projected to shrink by 53% to 70% during this century due to global climate change. However, the impact of future precipitation change on glacier change remains uncertain because mesoscale meteorology is not represented in current glacier models. We explore the effects of future changes in air temperature and precipitation by simulating the evolution of a benchmark glacier in the monsoon-influenced Nepal Himalaya using mesoscale climate-glacier modelling. Historical warming commits Khumbu Glacier to volume loss of 10–23% by 2100 CE. We show that while moderate future warming (RCP4.5) will lead to glacier volume loss of 70% by 2100 CE, the projected concurrent increase in precipitation will offset 34% of this change. However, extreme future warming (RCP8.5) will not be compensated by precipitation but will instead result in substantial ablation above 6,000 m and cause the highest glacier on Earth to vanish by 2160–2260 CE.

Projecting glacier change is critical for determining the impact of anthropogenic warming on regional water availability[1]. However, projections remain challenging because accumulation and ablation in mountain environments are driven by orographic feedbacks between high-relief topography and atmospheric circulation systems such as the South Asian Summer Monsoon[2]. High Mountain Asia is projected to lose 34 ± 19% of glacier ice by 2100 CE if warming is limited to 1.5°C to meet the ambitious Paris Agreement target[3]. More realistic glacier loss projections are 53 ± 23% under the moderate warming scenario RCP4.5 and 69 ± 20% under the extreme warming scenario RCP8.5[3–5]. In the monsoon-influenced Himalaya, changes in the extent and intensity of the Indian Summer Monsoon affected glacier expansion during the Last Glacial Maximum through changes in snowfall[6,7]. Global Climate Models project increasing Indian Summer Monsoon precipitation and variability with current global warming[8]. However, the effects of future changes in the Indian Summer Monsoon on glaciers in the Central and Eastern Himalaya in terms of precipitation amount, timing, and state (snow/rain) remain poorly understood[9–13].

We use a novel climate-glacier modelling approach to simulate the evolution of Khumbu Glacier (Fig. 1) from the present day (2015 CE) until 2300 CE. Khumbu Glacier is a benchmark glacier in the monsoon-influenced Himalaya and the highest glacier on Earth, flowing from 7981 m to 4879 m, which is representative of the majority of glaciers in the Central and Eastern Himalaya (Fig. 1b). We used downscaled Regional Climate Model (RCM) outputs with a surface energy balance model to force a glacier evolution model (Fig. 2a). To address the significant uncertainties associated with projections of climate change in the monsoon-influenced Himalaya, in particular, precipitation change, we made an ensemble experiment forced by three RCMs using two time slices (2015–2020 CE and 2095–2100 CE) downscaled using quantile mapping. The RCMs represent a range of possible future climates—the NOAA RCM is characterised by the highest annual precipitation, the IPSL RCM is characterised by the lowest annual precipitation, and the CCCma RCM is characterised by an intermediate value. Three downscaled RCMs under two future climate scenarios (RCP4.5 and RCP8.5)[14] were used as inputs to the surface energy balance model COSIPY[15] that includes sublimation of snow and ice, which are important, but overlooked, contributions to glacier mass balance in the Himalaya[16]. We used these six future mass balances to force the glacier model iSOSIA[17,18] from the present day to 2100 CE. iSOSIA is a higher-order ice flow model that includes two processes important for many Himalayan glaciers—the redistribution of snow by avalanching that is estimated to provide 75% of glacier accumulation, and the formation of supraglacial debris layers that insulate the ice surface and significantly modify ablation[17,19] (Fig. 1d).

Glacier change projections are complicated by supraglacial debris, which covers 4–7% of glacier surfaces globally[5,20] and 30% of glacier ablation areas in the Himalaya[3] (Fig. 1b). While satellite observations across the Himalaya show that rates of loss have accelerated over the last 40 years for both clean-ice glaciers and debris-covered glaciers[21], observations and models show that thick supraglacial debris slows glacier loss[5,22,23]. Projections of glacier evolution in the Himalaya are complicated by the need to account for the feedbacks between debris transport, mass balance, and ice flow[24] that promote a longer dynamic response to forcing compared to climatically equivalent clean-ice glaciers[17]. Many large Himalayan glaciers that are debris-covered are in greater imbalance with climate than clean-ice glaciers, sustaining more extensive ice volumes than would be possible without supraglacial debris. However, when a glacier is subject to an increasingly negative mass balance, the ice volume shrinks and ice flow declines towards the margins, and the lower part of the ablation area detaches from the active glacier[25]. This process of detachment and decay of the former ablation area is extended in time for debris-covered glaciers by the insulation of the ice surface, such that the new terminus of the active glacier initially remains in contact with the detached ice tongue rather than receding upvalley[23,26,27]. The proportion of debris-covered glacier area in the Himalaya means that these processes significantly affect projections of glacier change in this region, and yet few glacier modelling studies consider their impact[5].

Our transient climate-glacier model experiments (Fig. 2a) start with spin-up simulations of Khumbu Glacier that run from the late Holocene (0 CE) to the present day (2015 CE) under each of the three RCMs. This approach captures the present-day mass balance and dynamic state of the glacier and the distribution of englacial and supraglacial debris (Fig. 3). In considering the present state of Khumbu Glacier, we simulate the active glacier and assign the detached tongue to the model domain as a topographic feature[23,28–30]. The simulated glacier is evaluated against a range of observations, and the simulation forced using the NOAA RCM is identified as the starting point for future simulations. In the future simulations, local mean annual air temperatures (MAAT) in the Khumbu Valley increase by 1.4 ± 0.4°C under RCP4.5 and 3.8 ± 0.2°C under RCP8.5 by 2100 CE relative to the present day[31]. Greater warming occurs in winter than in summer under both RCPs[31] and results in an increase in annual precipitation amount of ~15%, with a greater increase in winter than in summer. There are no regional temperature projections beyond 2100 CE and therefore we use global values: between 2100 CE and 2200 CE a step change in warming for each of the 3 RCMs of 0.5°C for RCP4.5 and 2.8°C for RCP8.5 relative to 2100 CE is applied to simulate mass balance for 2200 CE, which is consistent with our time slice approach for the 21st Century simulations. Between 2200 CE and 2300 CE warming of 0.7°C for RCP4.5 and 4.1°C for RCP 8.5 relative to 2100 CE is applied to simulate mass balance for 2300 CE. There are no global projections of precipitation beyond 2100 CE and therefore no change in precipitation was applied beyond 2100 CE (see Supplementary Information for detailed experimental design and model evaluations).

Results

Climate change and glacier evolution from the present day until 2100 CE

Khumbu Glacier is responding to historical climate change and would continue to shrink even if warming ceased today. Indeed, if we allow the spin-up experiment to reach equilibrium with the present-day NOAA RCM mass balance, the glacier terminus will recede by 2.1 km and the maximum ice thickness will decrease from 246 m to 206 m by 2100 CE without any additional warming (Fig. 4a). Supraglacial debris up to 1.3 m thick extends 1 km up-glacier from the terminus and dampens this committed loss by sustaining 13% more ice volume than would be the possible for a clean-ice surface. The committed loss due to historical warming is 10–23% of the present-day glacier volume (Fig. 4b).

The mean glacier volume loss by 2100 CE across the RCM ensemble is 0.399×10^6 m^3 (46%) under RCP4.5 and 0.506×10^6 m^3 (57%) under RCP8.5. In the NOAA RCP4.5 experiment, glacier volume decreases by 36% between the present day and 2100 CE (Figs. 4 and 5). While significant, this end-of-century glacier loss is partially offset by the concurrent increase in precipitation. In comparison, an equivalent simulation forced only by warming of 1.4°C without any change in precipitation results in a more linear trajectory and 70% loss by 2100 CE (Fig. 5b), demonstrating that 34% of potential glacier loss resulting from warming air temperatures will be compensated by increasing precipitation. The CCCma RCP4.5 experiment projects loss of 57% by 2100 CE owing to a smaller increase in precipitation. In the NOAA RCP4.5 experiment, MAAT warms by 1.4°C by 2100 CE to reach –0.75°C, compared to warming of 1.6°C for the IPSL experiment and 2.2°C for the CCCma experiment. The NOAA experiment shows an increase in precipitation amount of 15% (from 581 mm to 665 mm) with the largest change occurring in winter. The resulting spatially averaged cumulative mass balance is –0.14 m water equivalent (w.e.) a^{-1} in 2100 CE; slightly more positive that the present-day value of –0.21 m w.e. a^{-1}. Therefore, keeping future warming within the limit of RCP4.5 will cause limit further shrinking of Khumbu Glacier to only 26% beyond that already committed to by historical climate change.

Under RCP8.5, all experiments give similar results for mass balance by 2100 CE with only a 10% difference in glacier volume between RCMs (Fig. 4b). For the NOAA RCP8.5 experiment, MAAT warms by 3.8°C by 2100 CE compared to 3.9°C for the IPSL experiment and 4.1°C for the CCCma experiment, and the 15% increase in annual precipitation is not sufficient to offset glacier loss (Fig. 4). The CCCma experiment has only a 1% difference in volume loss between RCP4.5 and RCP8.5 by 2100 CE despite a 1.9°C difference in MAAT. This is a surprising result given the significant temperature difference but it can be attributed to the greater number of high-magnitude precipitation events that occur under RCP8.5 in combination with the small difference in winter temperatures between the two RCPs. Indeed, in the CCCma experiment under RCP4.5, maximum winter temperature is 1.7°C higher than for the other RCMs, resulting in ablation and rainfall during the winter.

Climate change and glacier evolution from 2100 CE until 2300 CE

Projections of climate change beyond 2100 CE are more uncertain than those for this century, but do give rise to a clear prognosis for Khumbu Glacier. In all RCP4.5 experiments (an increase in MAAT of 0.7°C between 2100 CE and 2300 CE) there is little change in glacier volume between 2200 CE and 2300 CE compared to the 2100 CE value regardless of the RCM forcing used (Fig. 4b). In the NOAA RCP4.5 experiment, the Khumbu icefall is maintained until 2300 CE such that ice continues to flow from the Western Cwm to below 6,000 m and the glacier remains in contact with the dynamically detached tongue. Therefore, under RCP4.5 Khumbu Glacier could reach a new dynamic equilibrium that maintains a sufficient ice thickness to protect against catastrophic mass loss for at least two centuries. However, in all RCP8.5 experiments (an increase in MAAT of 4.1°C between 2100 CE and 2300 CE) substantial glacier loss occurs after 2100 CE and Khumbu Glacier completely decays before 2300 CE. Physical detachment of the debris-covered tongue from the active glacier occurs around 2070 CE in the CCCma and IPSL experiments and around 2140 CE in the NOAA experiment (Fig. 6). We define the glacier to be stagnant at flow at rates less than 10 m a^{-1}, which is a conservative estimate of the uncertainty associated with observations of glacier velocities[32]. Accordingly, we consider Khumbu Glacier to no longer be a viable system at this point, since there is minimal throughput of mass. In the NOAA RCP8.5 experiment, the glacier area is 1.2 km^2 and the mean velocity reduces to 10 m a^{-1} in 2260 CE such that the glacier is no longer viable. Glacier breakdown occurs earlier for the CCCma and IPSL RCMs because loss due to warming is not compensated to the same magnitude by an increase in precipitation as that projected under RCP8.5 using the NOAA RCM.

Discussion

In the monsoon-influenced Himalaya, 85% of glacier area is located above 5,000 m and 21% is above 6000 m (Fig. 1b). Despite these high elevations, Himalayan glaciers are currently rapidly losing ice in response to climate change[21]. The active terminus of Khumbu Glacier is located at 5100 m and the equilibrium line altitude is at 5850 m meaning that Khumbu Glacier is representative of many Himalayan glaciers (Fig. 1). Our simulations show that development of supraglacial debris at the terminus reduces net loss (Fig. 4a) but otherwise the glacier surface is clean (Fig. 3). Therefore, while supraglacial debris sustains about 13% of additional glacier volume, the local mass balance gradient is a more important control on glacier change for both clean-ice glaciers and debris-covered Himalayan glaciers. Our results show that the mass balance of Khumbu Glacier is close to zero by 2100 CE under RCP4.5, although with somewhat different ice volumes remaining depending on the RCM used (Fig. 4b). Therefore, if climate change is limited to RCP4.5, Khumbu Glacier will lose about a third of its volume and recede to the base of the icefall with insignificant further change. In this scenario, Khumbu Glacier has a similar extent in 2100 CE to the active section of the present-day glacier (Fig. 6) and is at least one example of how monsoon-influenced Himalayan glaciers could persist into the future if global efforts are sufficient to mitigate anthropogenic climate change.

While we have considered the effects on mass balance of mesoscale meteorology, smaller scale processes operating close to the ice surface could also be important. Katabatic winds are suggested to explain a local 15-year decrease in maximum air temperature and precipitation over glaciers while minimum air temperatures continue to rise[33]. However, the impact of micro-scale near-surface cooling on the duration and extent of mesoscale precipitation and accumulation is likely to be minimal, and unlikely to significantly affect mass balance[34,35]. Observations from an automatic weather station at Khumbu Glacier (6464 m) indicate that surface energy fluxes may be sufficient to cause non-negligible melting of glacier surfaces despite freezing air temperatures[36]. Results from an ice core from South Col Glacier (>8,000 m) combined with COSIPY experiments suggest that ablation may also take place at even at the highest elevations[37]. However, a subsequent study of the same glacier found no evidence of change and identified large uncertainties associated with simulating mass balance at these extreme elevations where sub-daily air temperature gradients and the duration of snow cover strongly affect ablation and accumulation[38]. Our results show that avalanching and sublimation are important controls on recent and future glacier evolution. Our study addresses these finer-scale temporal (hourly) and spatial (100 m) processes that affect glacier mass balance across the elevation range of Khumbu Glacier, but further observations of meteorological and glaciological conditions at the highest elevations would be beneficial[10,12,38,39].

The dynamic response of large glaciers to climate change is of the order of centuries, and significant changes in glacier volume continue after an imposed forcing ceases. For this reason, we start our simulations from 1.3 ka—when Khumbu Glacier was last considered dynamically stable[17,40]. The relationship between response time and mass balance becomes less important after 2100 CE when the glacier is so small that any dynamic behaviour has little impact on volume change. Previous glacier modelling studies start in the current century (e.g., 2000–2007 CE[4] or 2015[5]) and do not account for the committed dynamic response. A further complication arises from the use of global glacier inventories as a starting point for glacier modelling studies, as such inventories cannot capture the current dynamic state of glaciers that are imbalanced, and so include all ice-covered areas rather than identifying actively flowing ice. However, satellite-derived velocity products do identify where ice flow within glacier outlines declines to negligible rates[32]. The RGI 7.0 inventory for Khumbu Glacier is based on imagery from 1999 CE[41] where the detached debris-covered tongue represents 20% of the glacier volume contained within this outline (Fig. 1c). Comparison of present-day simulations with observations of recent changes in ice thickness and velocity through the ablation area below the icefall confirm that ice does not now flow into the stagnant tongue from the icefall[23] (see Supplementary Information for these results).

Comparing our results to those for the same glacier from a global modelling study forced by an ensemble of 10 Global Climate Models[5] shows that our experiments project less severe rates of ice volume decline resulting in a smaller amount of loss by 2100 CE (Fig. 5). In our experiments, there is 39% less loss under RCP4.5 and 32% less under RCP8.5 than in the global study. One difference between these results is that rather than using the global glacier inventory outline to define the glacier margins we consider only the actively flowing glacier and so exclude 20% of the starting glacier volume in the detached tongue. We would expect the two sections of the glacier to evolve along different paths: while the active glacier responds to climate change as projected in our experiments, thick supraglacial debris mantling the detached tongue could allow this ice mass to survive and slowly decay *in situ* for many decades beyond the present day. The decay of the detached tongue may however increase due to erosion of the surface by ice cliffs and supraglacial water bodies that are expanding across the former glacier surface.

Current global greenhouse gas emissions are following the trajectory of the moderate warming scenario RCP4.5, and the extreme warming scenario RCP8.5 could be described as 'low-possibility but high-impact'[42]. However, mountain regions are warming more rapidly than the global mean[43] such that a global temperature rise of 1.5°C will lead to 2.1 ± 0.1°C of warming in High Mountain Asia[3,43] (although the occurrence of elevation-dependent warming above 5,000 m is debated[44]). High-magnitude precipitation events from winter Westerly disturbances increased by up to a factor of seven between the present day and 2100 CE under RCP8.5, and could make the net annual mass balance less negative than would be the case when solely forced by change in MAAT. We found no evidence of future increases in precipitation offsetting RCP8.5 warming—net glacier mass balance was strongly negative in all RCP8.5 experiments and insufficient to maintain actively flowing glaciers. Under RCP8.5, glacier mass balance in the monsoon-influenced Himalaya may therefore shift from being driven by accumulation during the monsoon to predominantly during winter, with monsoon precipitation only resulting in snow accumulation at the very highest elevations being insufficient to maintain flowing glaciers. This outcome is avoidable by limiting anthropogenic warming to within the RCP4.5 scenario, which, due to the associated increase in precipitation, could sustain nearly two thirds of the current glacier volume until 2100 CE and potentially a two centuries further into the future.

Online Methods

Regional climate model (RCM) downscaling

Downscaled RCMs were used to calculate the present day and future mass balances used as inputs to the glacier model. Daily data from the Coordinated Regional Downscaling Experiment (CORDEX) South Asia domain were downloaded from the Indian Institute of Tropical Meteorology website (http://cccr.tropmet.res.in/home/cordexsa_about.jsp) for the grid box nearest to Khumbu Glacier (27.9065°N, 86.4353°E). Incoming shortwave and longwave radiation components were downloaded from the ESGF portal (https://esgf-ui.ceda.ac.uk/cog/projects/cordex-ceda/). Three RCMs were chosen to span the range of possible precipitation future scenarios and subject to quantile mapping to force separate glacier mass balance calculations. Observational data from automatic weather stations (Fig. 1c) collected between January 2006 and November 2019 by Ev-K2-CNR and GlacioClim (https://glacioclim.osug.fr/) were used to aid RCM downscaling with gaps filled with interpolated data from neighbouring stations where possible (Fig. 2). The automatic weather station data were used to disaggregate daily downscaled present-day and end-of-century climate data to an hourly resolution[45] using seasonal means to reproduce the 'nocturnal peak' seen during the monsoon. The MELODIST Python tool was used for all other meteorological variables[46].

The climate time slice for the period 2095–2100 CE was used to force the future mass balance simulations and drive the ice-flow model from the present-day simulation. Time slices representing five-year periods were chosen to reduce the computational expense of the climate-glacier modelling (~24 hours per simulation) and the preceding decade was used for comparison with the climate time slices. The climate forcing for the downscaled NOAA RCM under RCP 4.5 was 1.4°C higher than present day (MAAT of –0.75°C in 2095–2100 CE compared with –2.15°C in 2015–2020 CE). Annual precipitation increased by 14.8% from 581.4 mm in the present day to 664.8 mm a^{-1} in 2100 CE under RCP4.5, of which summer (JJAS) precipitation increased by 5.4% and winter (DJF) precipitation increased by 14.1%. The climate forcing for the downscaled NOAA RCM under RCP 8.5 was 3.8°C higher than present day (MAAT of 1.65°C in 2095–2100 CE). Annual precipitation increased by 14.9% in 2100 CE under RCP8.5, of which summer precipitation increased by 9.8% and winter precipitation increased by 19.4%.

Surface energy and mass balance modelling using COSIPY

The Coupled Snowpack and Ice-surface Energy and Mass Balance model in Python (COSIPY) was used to calculate surface energy balance[15]. This model has been applied to a range of mountain glaciers including those in High Mountain Asia[38,47]. COSIPY is developed and modularised in Python and integrates a surface energy balance model with a multi-layer snow and ice model and thereby resolves all energy fluxes at the ice surface that contribute to surface melt. COSIPY includes a calculation of sublimation, which is an important ablation process for high-elevation glaciers in the Himalaya[48].

The model domain was a 30-m digital elevation model acquired from the Shuttle Radar Topography Mission[49] resampled to 100-m grid spacing. We used the topographic rather than subglacial surface to calculate annual clean-ice glacier surface mass balance to enable integration with the glacier model by making the domain for the mass balance calculations larger than the glacier area. COSIPY was forced by hourly meteorology with nine parameters to calculate the energy balance and mass balance components at an hourly time step from the sum of accumulation by solid precipitation, deposition, and refreezing of melt water percolation, and ablation by melt and sublimation. The impact of supraglacial debris on ablation rates and avalanching on accumulation rates was handled subsequently in the glacier model.

Glacier evolution modelling using iSOSIA

The integrated second-order shallow ice approximation model (iSOSIA) is a 3-D depth-integrated, higher-order ice-dynamical glacier evolution model that solves for the flow of ice including longitudinal and transverse stress gradients that are imposed on ice flow through high-relief topography[18]. iSOSIA has a variable time step that can adjust to allow greater computational efficiency to a maximum of 0.1 years. The glacier model was developed to simulate the evolution of debris-covered glaciers by incorporating the feedbacks between debris transport, mass balance, and ice flow[17].

The glacier model parameterisation and experimental design followed our previous work[23]. Estimated ice thickness[50] was subtracted from the 30-m digital elevation model to yield a subglacial topography for the model domain. The ice-free model domain incorporates the full hydrological catchment and includes the steep hillslopes of the Western Cwm that provide snow by avalanching to the glacier surface. The total amount of snow accumulation across that catchment was calibrated such that the snow delivered to the glacier surface was equivalent to the estimated rate of glacier accumulation of about 2 m water equivalent per year[51]. Avalanching was simulated by removing snow and ice from hillslopes greater than 28° and redistributing this mass across less steep surfaces using a non-linear hillslope flux model[52]. The avalanching routine was previously applied to Khumbu Glacier and found to be sufficient to prevent snow and ice accumulation on slopes that are observed to be free of glacier ice such as the southwest face of Sagarmatha (Mt. Everest) whilst allowing accumulation on steep sections of the glacier[17].

Debris was delivered to the glacier surface from headwall erosion using a similar non-linear hillslope flux model to the avalanching routine. Debris was produced by erosion from hillslopes without ice at a constant rate of 1 mm a^{-1}. The reduction in ablation beneath supraglacial debris from clean-ice values was represented as a reciprocal function that scales clean-ice ablation (b_{clean}) to give sub-debris melt (b_{debris}) as a function of debris thickness (h):

$$b_{debris} = b_{clean} \times \frac{h_0}{h + h_0} \qquad \text{Eq(1)}$$

where h_0 is a constant representing the characteristic debris thickness at which the reduction in ablation due to insulation by supraglacial debris is 50% of the value for an equivalent clean-ice surface. The value for h_0 of 0.8 m represents a positively skewed supraglacial debris thickness distribution that includes ablation 'hotspots' such as supraglacial ponds and ice cliffs and is representative of the current state of Khumbu Glacier[23]. Observations and modelling of the dynamics and structure of Khumbu Glacier show that the lower 5 km (25% of the total length, 20% of total ice volume) is stagnant and dynamically detached from the active glacier in the last 100 years[23,27]. Basal ice at the glacier surface indicates that the active terminus overrides the stagnant tongue[28] and surface displacement measurements indicate that ice no longer flows longitudinally through the detached debris-covered tongue and is instead collapsing laterally at 3 m a^{-1},[30]. The simulated active glacier matches observed changes in the spatial distribution of surface debris[29] and feature-tracking and remote-sensing observations of surface elevation change[22]. We therefore simulated the active glacier and assign the former debris-covered tongue to the model domain as a static topographic feature.

Figures and captions

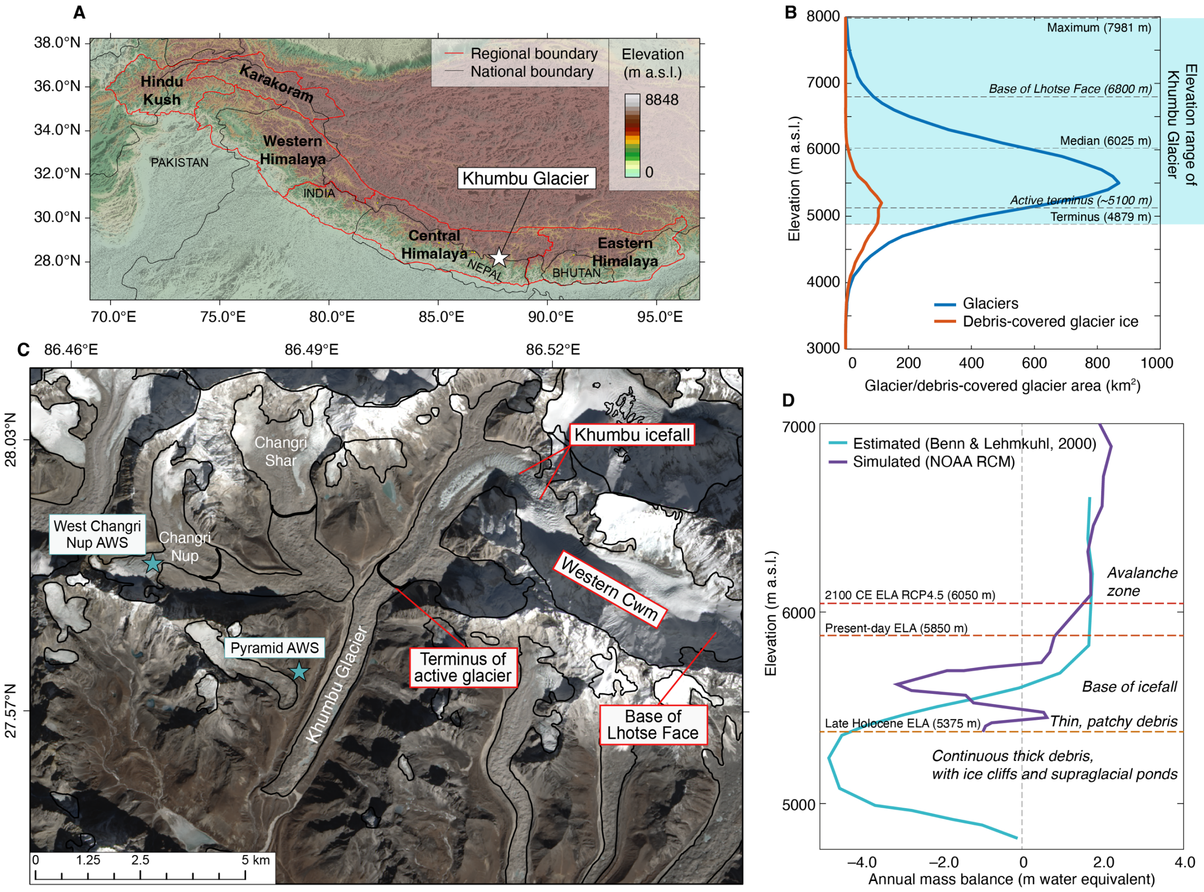

Figure 1: Khumbu Glacier location and context. (a) Location map of High Mountain Asia showing the location of the monsoon-influenced Central and Eastern Himalaya and Khumbu Glacier. (b) hypsometry of glaciers and debris-covered glacier ice in the Central and Eastern Himalaya compared with the elevations of Khumbu Glacier. (c) Satellite image of Khumbu Glacier showing the extent of supraglacial debris, location of the icefall, the extent of active ice flow inferred from observations of glacier velocity (black lines) and location of the automatic weather stations used for RCM downscaling (blue stars). (d) Estimated mass balance gradient for debris-covered glaciers in the Everest region[51] compared with the glacier mass balance gradient simulated using the NOAA RCM and showing change in the equilibrium line altitude (ELA) of Khumbu Glacier in the historical and future simulations for the NOAA RCP4.5 experiment.

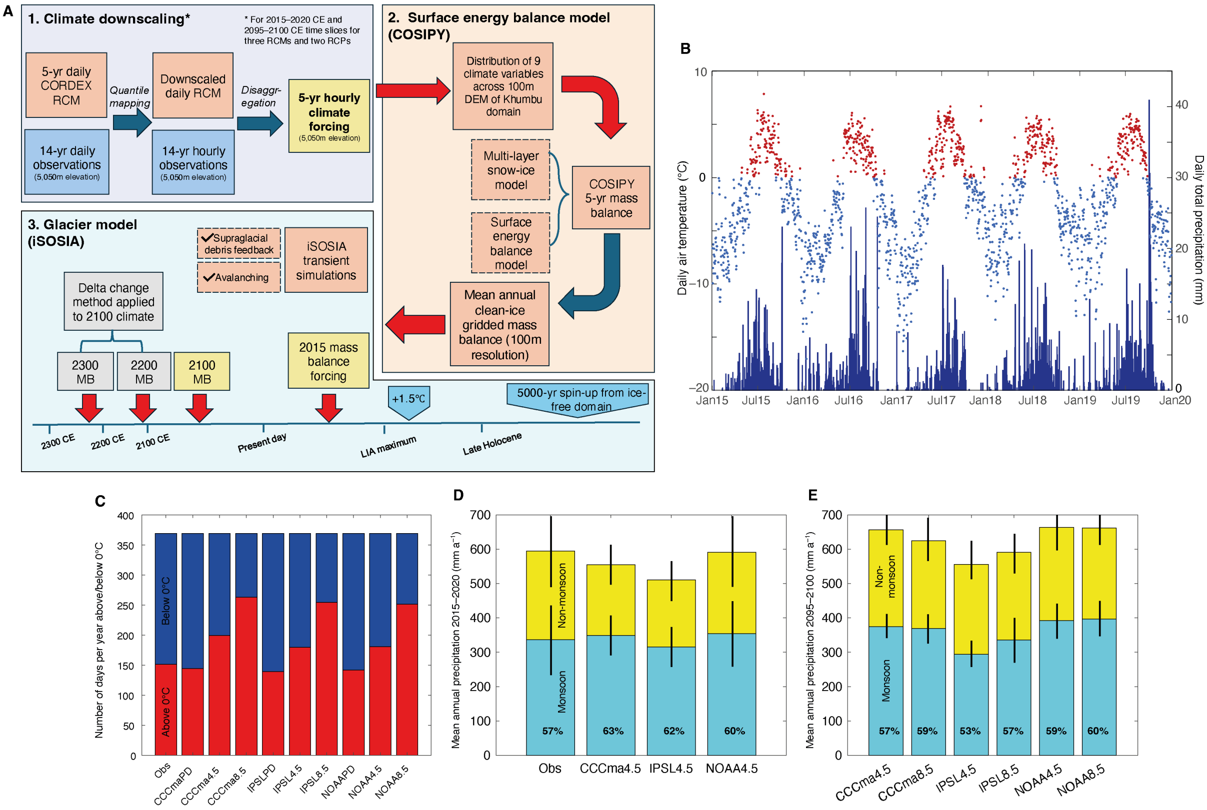

Figure 2: Model experimental design and evaluation of RCM downscaling. (a) Schematic diagram of the climate-glacier modelling approach showing the methods used for downscaling through quantile mapping and disaggregation of climate data. Note that this process does not apply to the post-2100 CE climate forcings which are subject to delta change. Surface energy balance modelling using COSIPY includes the pre-processing stage of meteorological distribution across the Khumbu domain, which is repeated for each RCM in the 2015–2020 CE climates and for the three RCMs and two RCPs for the 2095–2100 CE climates, then used as input to the glacier model iSOSIA. (b) Daily mean temperature and daily total precipitation from the NOAA RCM for the present day (2015–2020 CE) following downscaling using quantile mapping with air temperature categorised into above freezing (red) and below freezing (blue). (c) Proportion of air temperatures above and below freezing for the present day for each RCM and RCP for the downscaled daily data compared with observations. (d) Annual precipitation totals for non-monsoon and monsoon with standard deviation between selected years shown by black bars for the downscaled daily data compared with observations. (e) Future (2095–2100 CE) time-slice annual precipitation totals for non-monsoon and monsoon months with standard deviation between selected years shown by black bars. In (d) and (e) the percentage of the total annual precipitation occurring during the monsoon is indicated by the value in bold text. (Obs = meteorological observations from AWS).

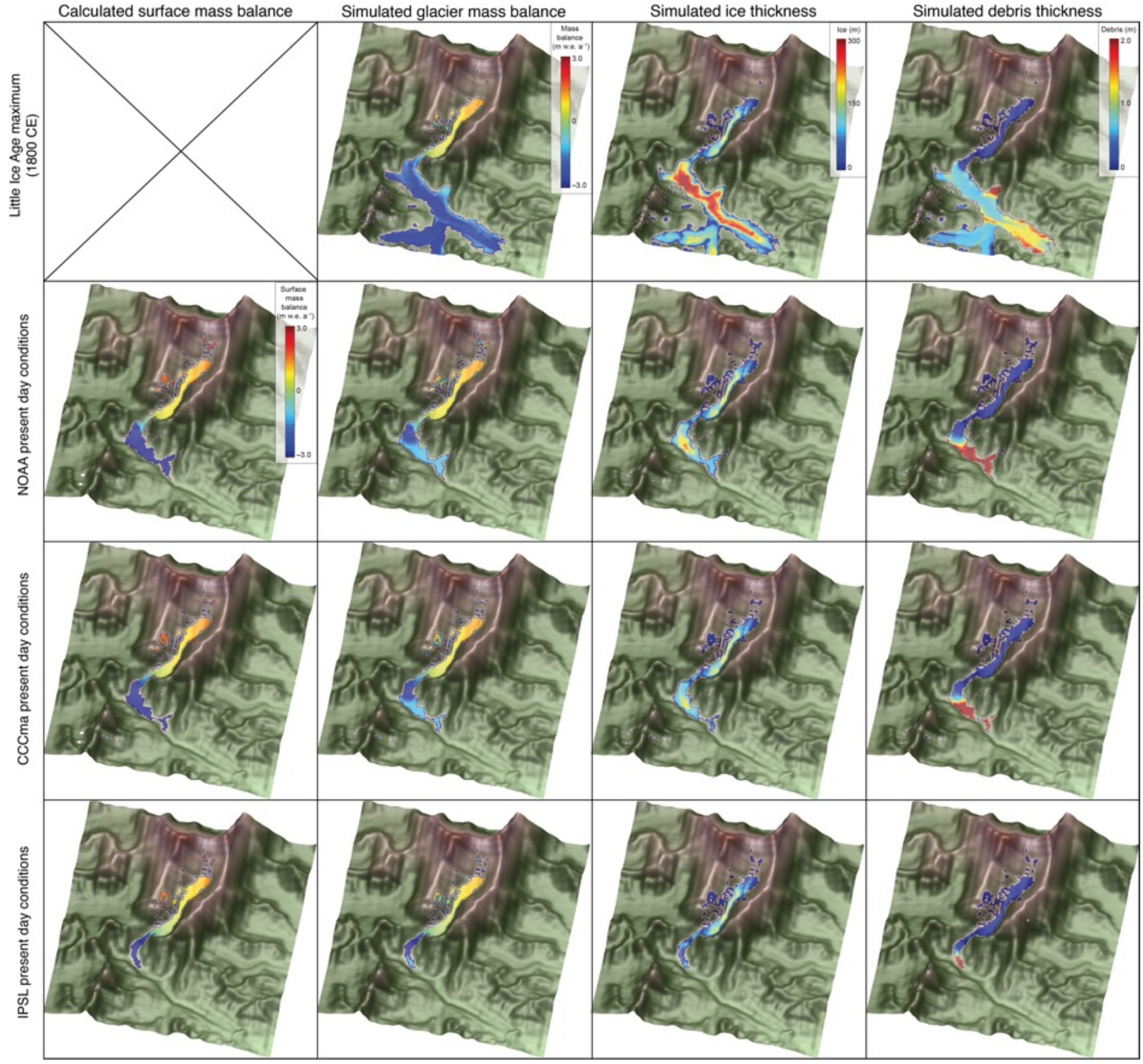

Figure 3. Glacier model sensitivity to surface energy and mass balance forcing, showing Little Ice Age (~1800 CE) glacier mass balance, ice thickness and debris thickness. Present-day results for surface mass balance calculated using each RCM with COSIPY showing glacier mass balance calculated using the same climate forcing following integration with iSOSIA, simulated ice thickness, and simulated debris thickness.

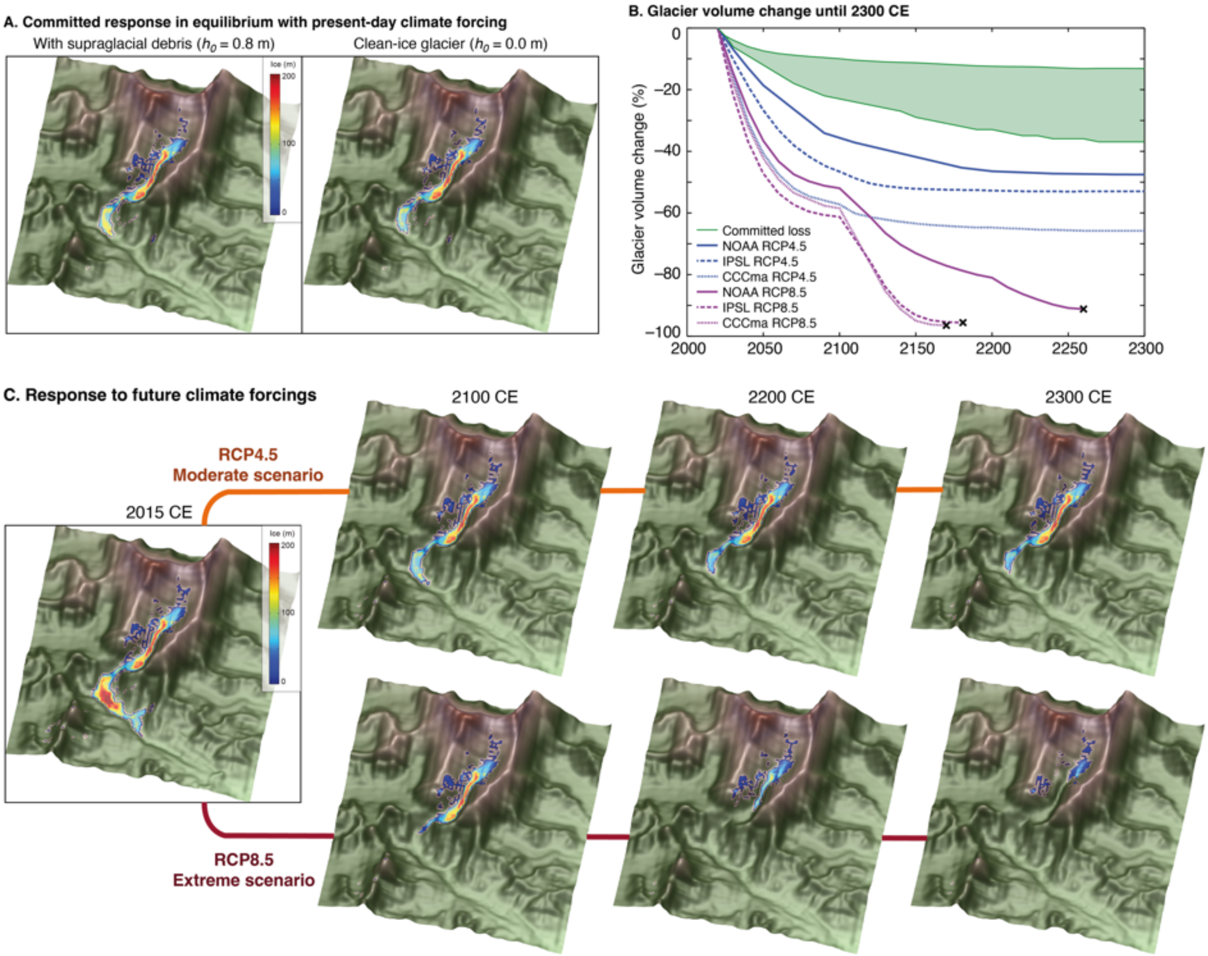

Figure 4. Future glacier volume change projections. (a) Equilibrium ice thickness accounting for the committed response to recent climate change using the downscaled NOAA climate forcing with and without the effect of sub-debris melt. (b) Simulated glacier volume change from the present day (2015–2020 CE) until 2300 CE under RCP4.5 and RCP8.5 for the three downscaled RCMs. The black crosses mark when ice flow has declined sufficiently that the glacier is considered almost absent or no longer viable. The green shading shows the range of the committed volume loss due to historical warming. (c) Simulated ice thickness under RCP4.5 and RCP8.5 for 2100 CE, 2200 CE and 2300 CE using the downscaled NOAA climate forcing.

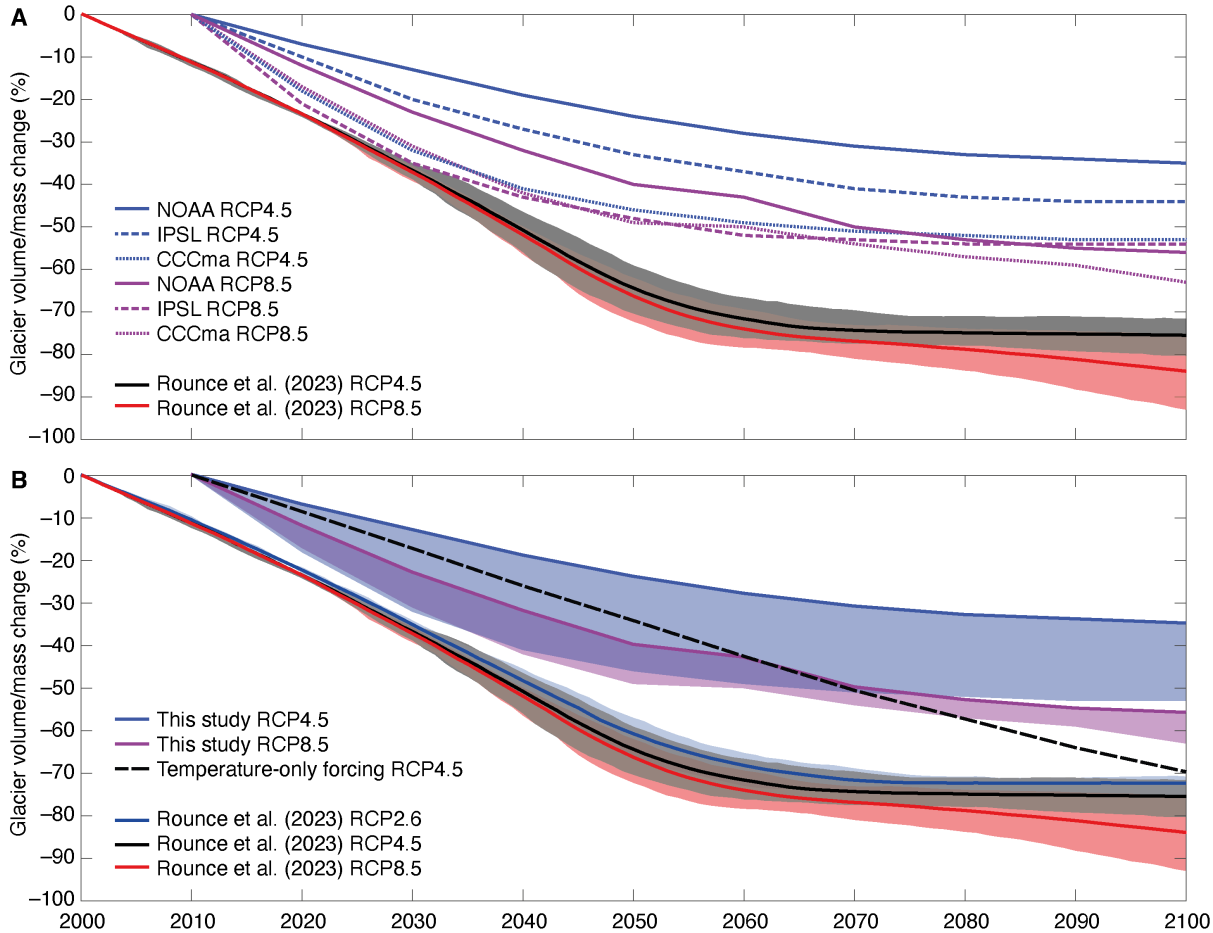

Figure 5. Comparison of projected shrinkage of Khumbu Glacier by 2100 CE from this study with those from Rounce et al. (2023) showing (a) results from each of the six experiments in this study with results from RCP4.5 and RCP8.5 from Rounce et al. (2023), and (b) comparison of results from this study where the bold line shows the NOAA RCP4.5 and RCP8.5 experiments and the black dashed line shows the equivalent result for a simulation where precipitation does not change from the present-day value compared with results from Rounce et al. (2023) for RCP2.6, RCP4.5 and RCP8.5.

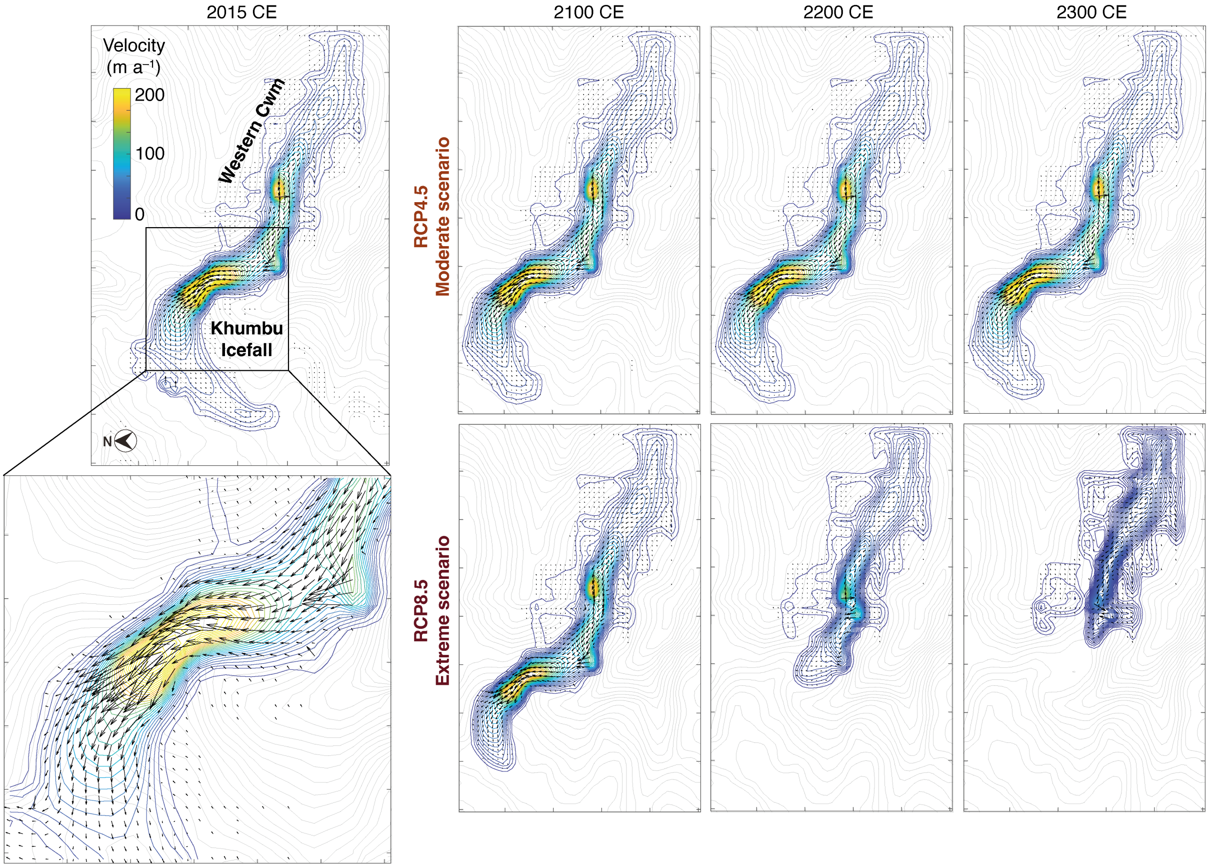

Figure 6. Simulated ice flow for Khumbu Glacier. Velocity-vector maps showing simulated ice flow magnitude and direction from the present day (2015–2020 CE) until 2300 CE under RCP4.5 and RCP8.5 using the downscaled NOAA climate forcing and a value for h_0 of 0.8 m. Simulated ice flow speed is shown as colour shading with blue contours, and the bed topography is shown by grey contours. The outermost contour in each plot represents the slowest ice flow close to the glacier margins with depth-integrated velocities of 5–10 m a^{-1}. Note that rapid flow across the Western Cwm indicated by one arrow shows the effects of avalanching rather than sustained glacier flow.

Acknowledgements

ASD was supported by the Priestley International Centre for Climate at the University of Leeds, and a University of Leeds Anniversary Research Scholarship. AVR was supported by a Royal Society Dorothy Hodgkin Research Fellowship (DHF\R1\201113). Tobias Sauter and Anselm Arndt are thanked for support in using COSIPY. We thank Patrick Wagnon for sharing the Pyramid and Changri Nup Glacier automatic weather station data. We thank David Rounce for sharing global glacier model results for Khumbu Glacier. Some of the simulations were performed on resources provided by Sigma2, the National Infrastructure for High-Performance Computing and Data Storage in Norway. The Editor, Associate Editor and three anonymous reviewers are thanked for their constructive and detailed comments on an earlier version of this manuscript.

Data Availability

All data used in this study are publicly available through the repositories listed in the Online Methods and Supplementary Information.

Code availability

The COSIPY surface energy balance model is publicly available through the repository listed in the online methods. The version of the glacier model iSOSIA used in this study is available from Zenodo: Ann Rowan. (2024). annvrowan/isosia: iSOSIA version used in Schlich-Davies et al. (spm-3.3.3r). Zenodo. https://doi.org/10.5281/zenodo.12666864

References

1. Pritchard, H. D. Asia's shrinking glaciers protect large populations from drought stress. *Nature* **569**, 649–654 (2019).
2. Bookhagen, B. & Burbank, D. W. Topography, relief, and TRMM-derived rainfall variations along the Himalaya. *Geophys. Res. Lett.* **33**, L08405 (2006).
3. Kraaijenbrink, P. D. A., Bierkens, M. F. P., Lutz, A. F. & Immerzeel, W. W. Impact of a global temperature rise of 1.5 degrees Celsius on Asia's glaciers. *Nature* **549**, 257–260 (2017).
4. Marzeion, B. *et al.* Partitioning the Uncertainty of Ensemble Projections of Global Glacier Mass Change. *Earth's Future* **8**, e2019EF001470 (2020).
5. Rounce, D. R. *et al.* Global glacier change in the 21st century: Every increase in temperature matters. *Science* **379**, 78–83 (2023).
6. Benn, D. I. & Owen, L. A. The role of the Indian summer monsoon and the mid-latitude westerlies in Himalayan glaciation: review and speculative discussion. *Journal of the Geological Society* **155**, 353–363 (1998).
7. Owen, L. A. *et al.* Quaternary glaciation of Mount Everest. *Quaternary Science Reviews* **28**, 1412–1433 (2009).
8. Katzenberger, A., Schewe, J., Pongratz, J. & Levermann, A. Robust increase of Indian monsoon rainfall and its variability under future warming in CMIP6 models. *Earth Syst. Dynam.* **12**, 367–386 (2021).
9. Immerzeel, W. W., van Beek, L. P. H., Konz, M., Shrestha, A. B. & Bierkens, M. F. P. Hydrological response to climate change in a glacierized catchment in the Himalayas. *Climatic Change* **110**, 721–736 (2012).
10. Mölg, T., Maussion, F. & Scherer, D. Mid-latitude westerlies as a driver of glacier variability in monsoonal High Asia. *Nature Climate Change* **4**, 68–73 (2014).
11. Ragettli, S., Immerzeel, W. W. & Pellicciotti, F. Contrasting climate change impact on river flows from high-altitude catchments in the Himalayan and Andes Mountains. *Proc Natl Acad Sci USA* **113**, 9222–9227 (2016).
12. Shaw, T. E. *et al.* Multi-decadal monsoon characteristics and glacier response in High Mountain Asia. *Environ. Res. Lett.* **17**, 104001 (2022).
13. Shea, J. M., Immerzeel, W. W., Wagnon, P., Vincent, C. & Bajracharya, S. Modelling glacier change in the Everest region, Nepal Himalaya. *The Cryosphere* **9**, 1105–1128 (2015).
14. Collins, M., Knutti, R., & Arblaster, J. Long-term Climate Change: Projections, Commitments and Irreversibility. In: Climate Change 2013: The Physical Science Basis. Contribution of Working Group I to the Fifth Assessment Report of the Intergovernmental Panel on Climate Change [Stocker, T.F., D. Qin, G.-K. Plattner, M. Tignor, S.K. Allen, J. Boschung, A. Nauels, Y. Xia, V. Bex and P.M. Midgley (eds.)]. Cambridge University Press, Cambridge, United Kingdom and New York, NY, USA,, 1–108. (2013).
15. Sauter, T., Arndt, A. & Schneider, C. COSIPY v1.3 – an open-source coupled snowpack and ice surface energy and mass balance model. *Geosci. Model Dev.* **13**, 5645–5662 (2020).
16. Stigter, E. E. *et al.* The Importance of Snow Sublimation on a Himalayan Glacier. *Front. Earth Sci.* **6**, 108 (2018).
17. Rowan, A. V., Egholm, D. L., Quincey, D. J. & Glasser, N. F. Modelling the feedbacks between mass balance, ice flow and debris transport to predict the response to climate change of debris-covered glaciers in the Himalaya. *Earth and Planetary Science Letters* **430**, 427–438 (2015).
18. Egholm, D. L., Knudsen, M. F., Clark, C. D. & Lesemann, J. E. Modeling the flow of glaciers in steep terrains: The integrated second-order shallow ice approximation (iSOSIA). *J. Geophys. Res. Earth Surf.* **116**, (2011).
19. Anderson, L. S. & Anderson, R. S. Modeling debris-covered glaciers: response to steady debris deposition. *The Cryosphere* **10**, 1105–1124 (2016).
20. Herreid, S. & Pellicciotti, F. The state of rock debris covering Earth's glaciers. *Nat. Geosci.* **13**, 621–627 (2020).
21. Maurer, J. M., Schaefer, J. M., Rupper, S. & Corley, A. Acceleration of ice loss across the Himalayas over the past 40 years. *Sci. Adv.* **5**, eaav7266 (2019).
22. King, O. *et al.* Six Decades of Glacier Mass Changes around Mt. Everest Are Revealed by Historical and Contemporary Images. *One Earth* **3**, 608–620 (2020).

23. Rowan, A. V. *et al.* The Role of Differential Ablation and Dynamic Detachment in Driving Accelerating Mass Loss From a Debris-Covered Himalayan Glacier. *J. Geophys. Res. Earth Surf.* **126**, (2021).
24. Nicholson, L., Wirbel, A., Mayer, C. & Lambrecht, A. The Challenge of Non-Stationary Feedbacks in Modeling the Response of Debris-Covered Glaciers to Climate Forcing. *Front. Earth Sci.* **9**, 662695 (2021).
25. Rippin, D. M., Sharp, M., Van Wychen, W. & Zubot, D. 'Detachment' of icefield outlet glaciers: catastrophic thinning and retreat of the Columbia Glacier (Canada). *Earth Surf. Process. Landforms* **45**, 459–472 (2020).
26. Pellicciotti, F. *et al.* Mass-balance changes of the debris-covered glaciers in the Langtang Himal, Nepal, from 1974 to 1999. *J. Glaciol.* **61**, 373–386 (2015).
27. Quincey, D. J., Luckman, A. & Benn, D. Quantification of Everest region glacier velocities between 1992 and 2002, using satellite radar interferometry and feature tracking. *J. Glaciol.* **55**, 596–606 (2009).
28. Miles, K. E. *et al.* Continuous borehole optical televiewing reveals variable englacial debris concentrations at Khumbu Glacier, Nepal. *Commun Earth Environ* **2**, 12 (2021).
29. Nakawo, M. Processes Which Distribute Supraglacial Debris On The Khumbu Glacier, Nepal Himalaya. *Ann. Glacio*. **8**, 129–131 (1986).
30. Watson, C. S. *et al.* Quantifying ice cliff evolution with multi-temporal point clouds on the debris-covered Khumbu Glacier, Nepal. *J. Glaciol.* **63**, 823–837 (2017).
31. Sanjay, J., Krishnan, R., Shrestha, A. B., Rajbhandari, R. & Ren, G.-Y. Downscaled climate change projections for the Hindu Kush Himalayan region using CORDEX South Asia regional climate models. *Advances in Climate Change Research* **8**, 185–198 (2017).
32. Dehecq, A. *et al.* Twenty-first century glacier slowdown driven by mass loss in High Mountain Asia. *Nature Geosci* **12**, 22–27 (2019).
33. Salerno, F. *et al.* Local cooling and drying induced by Himalayan glaciers under global warming. *Nat. Geosci.* **16**, 1120–1127 (2023).
34. Mott, R., Stiperski, I. & Nicholson, L. Spatio-temporal flow variations driving heat exchange processes at a mountain glacier. *The Cryosphere* **14**, 4699–4718 (2020).
35. Shaw, T. E., Buri, P., McCarthy, M., Miles, E. S. & Pellicciotti, F. Local Controls on Near-Surface Glacier Cooling Under Warm Atmospheric Conditions. *JGR Atmospheres* **129**, e2023JD040214 (2024).
36. Matthews, T. *et al.* Going to Extremes: Installing the World's Highest Weather Stations on Mount Everest. *Bulletin of the American Meteorological Society* **101**, E1870–E1890 (2020).
37. Potocki, M. *et al.* Mt. Everest's highest glacier is a sentinel for accelerating ice loss. *npj Clim Atmos Sci* **5**, 7 (2022).
38. Brun, F. *et al.* Everest South Col Glacier did not thin during the period 1984–2017. *The Cryosphere* **17**, 3251–3268 (2023).
39. Khadka, A. *et al.* Weather on Mount Everest during the 2019 summer monsoon. *Weather* **76**, 205–207 (2021).
40. Hornsey, J. *et al.* Be-10 Dating of Ice-Marginal Moraines in the Khumbu Valley, Nepal, Central Himalaya, Reveals the Response of Monsoon-Influenced Glaciers to Holocene Climate Change. *JGR Earth Surface* **127**, (2022).
41. RGI 7.0 Consortium. A Dataset of Global Glacier Outlines, Version 7.0. Boulder, Colorado USA. NSIDC: National Snow and Ice Data Center. https://doi.org/10.5067/f6jmovy5navz (2023).
42. Pedersen, J. S. T. *et al.* Variability in historical emissions trends suggests a need for a wide range of global scenarios and regional analyses. *Commun Earth Environ* **1**, 41 (2020).
43. Pepin, N. C. *et al.* Climate Changes and Their Elevational Patterns in the Mountains of the World. *Reviews of Geophysics* **60**, (2022).
44. Gao, Y. *et al.* Does elevation-dependent warming hold true above 5000 m elevation? Lessons from the Tibetan Plateau. *npj Clim Atmos Sci* **1**, 19 (2018).
45. Debele, B., Srinivasan, R. & Yves Parlange, J. Accuracy evaluation of weather data generation and disaggregation methods at finer timescales. *Advances in Water Resources* **30**, 1286–1300 (2007).

46. Förster, K., Hanzer, F., Winter, B., Marke, T. & Strasser, U. An open-source MEteoroLOgical observation time series DISaggregation Tool (MELODIST v0.1.1). *Geosci. Model Dev.* **9**, 2315–2333 (2016).
47. Huintjes, E., Neckel, N., Hochschild, V. & Schneider, C. Surface energy and mass balance at Purogangri ice cap, central Tibetan Plateau, 2001–2011. *J. Glaciol.* **61**, 1048–1060 (2015).
48. Bonekamp, P. N. J., Wanders, N., Wiel, K., Lutz, A. F. & Immerzeel, W. W. Using large ensemble modelling to derive future changes in mountain specific climate indicators in a 2 and 3°C warmer world in High Mountain Asia. *Int J Climatol* **41**, (2021).
49. Farr, T. G. *et al.* The Shuttle Radar Topography Mission. *Reviews of Geophysics* **45**, 2005RG000183 (2007).
50. Farinotti, D. *et al.* A consensus estimate for the ice thickness distribution of all glaciers on Earth. *Nat. Geosci.* **12**, 168–173 (2019).
51. Benn, D. I. & Lehmkuhl, F. Mass balance and equilibrium-line altitudes of glaciers in high-mountain environments. *Quaternary International* **65–66**, 15–29 (2000).
52. Roering, J. J., Kirchner, J. W. & Dietrich, W. E. Evidence for nonlinear, diffusive sediment transport on hillslopes and implications for landscape morphology. *Water Resources Research* **35**, 853–870 (1999).